

Supporting Information:

Tuning small electron polaron in FePO₄ by P-site or O-site doping based on DFT+U and KMC simulation

Taowen Chen¹, Yaokun Ye^{1,}, Ying Wang¹, Chi Fang¹, Weicheng Lin¹, Yao Jiang²,*

Bo Xu², Chuying Ouyang^{2,}, and Jiaxin Zheng^{1,2,*}*

¹School of Advanced Materials, Peking University, Shenzhen Graduate School,
Shenzhen 518055, People's Republic of China

²Fujian science & technology innovation laboratory for energy devices of China
(21C-LAB), Ningde 352100, People's Republic of China

AUTHOR INFORMATION

Corresponding Author

* Yaokun Ye, E-mail: yeyaokun@pku.edu.cn

* Chuying Ouyang, E-mail: ouyangcy@catl.com

* Jiaxin Zheng, E-mail: zhengjx@pkusz.edu.cn

Constants

- A. Schematic diagram of the hopping path.
- B. Lattice constant information by DFT+U calculation.
- C. Bader charge data of all systems.
- D. Bond length distortion when form polaron.
- E. All the data of E_{POL} .
- F. The data of Fe-O bond length at IS, TS, FS.
- G. The data of polaron hopping rate.
- H. Kinetic Monte Carlo simulation for small polaron hopping.

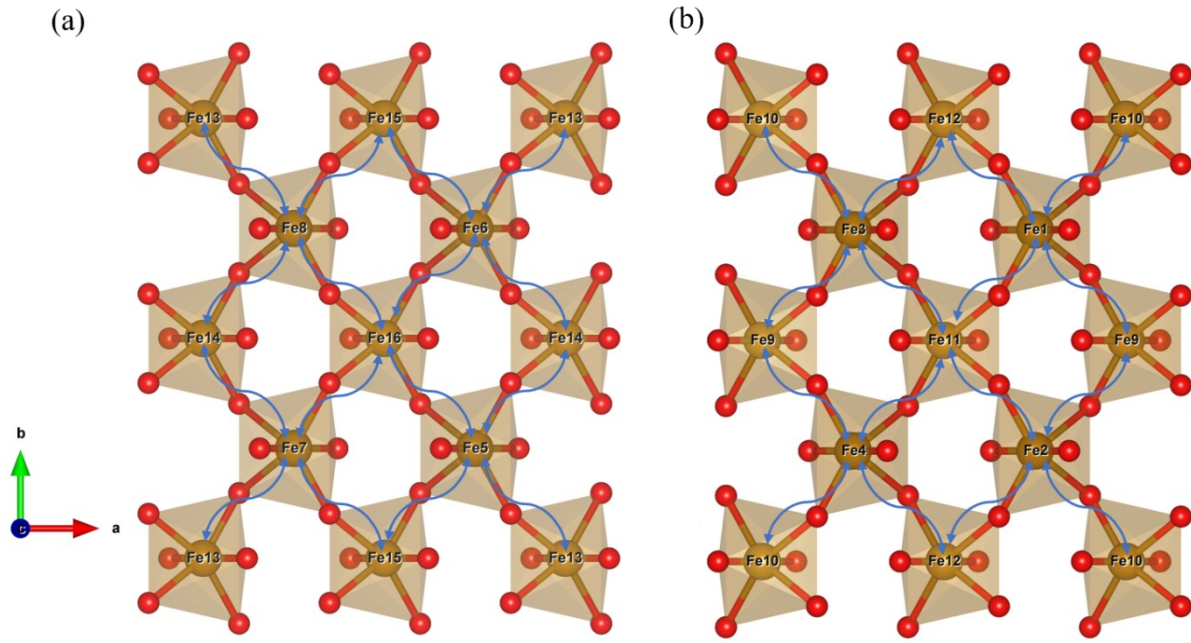


Figure S1: Schematic diagram of the hopping path. Only Fe-O octahedra are shown in the figure. Arrow curves indicate polarons can transition between two iron atoms. (a) The upper layer. (b) The lower layer.

A. Schematic diagram of the hopping path.

For the hopping pathways, we only considered the nearest-neighbor sites, as shown in Figure S1. For the pristine system, all the Fe sites are equivalent due to the crystal symmetry, so only one hopping between any two adjacent Fe atoms needs to be calculated. By contrast, each Fe atom in the doped systems is surrounded by four unequal nearest-neighbor Fe atoms, which means that all the hopping pathways between two adjacent Fe atoms need to be calculated.

In other words, there are a total of 64 hopping paths in total in each doped system, of which 32 are in the upper layer (Figure S1a) and 32 are in the lower layer (Figure S1b), including round-trip hop.

B. Lattice constant information by DFT+U calculation.

Table S1. The lattice constant of $2 \times 2 \times 1$ supercell in the pristine and doping systems by DFT+U calculation.

	a (Å)	b (Å)	c (Å)	α (°)	β (°)	γ (°)
$\text{Fe}_{16}\text{P}_{16}\text{O}_{64}$	9.765	11.845	9.977	90	90	90.001
$\text{Fe}_{16}(\text{PO}_4)_{15}\text{AsO}_4$	9.785	11.85	10.01	90	89.998	90
$\text{Fe}_{16}(\text{PO}_4)_{15}\text{SeO}_4$	9.706	11.742	9.94	90	90.057	90
$\text{Fe}_{16}(\text{PO}_4)_{15}\text{SO}_4$	9.688	11.733	9.911	90	90.045	90
$\text{Fe}_{16}(\text{PO}_4)_{15}\text{SiO}_4$	9.852	11.968	10.044	90	89.976	90
$\text{Fe}_{16}(\text{PO}_4)_{15}\text{VO}_4$	9.777	11.849	10.02	90	90.063	90
$\text{Fe}_{16}(\text{PO}_4)_{15}\text{PO}_3\text{S}$	9.818	11.900	9.987	89.770	90.225	89.689
$\text{Fe}_{16}(\text{PO}_4)_{15}\text{PO}_3\text{F}$	9.703	11.764	9.915	90.084	89.818	89.334
$\text{Fe}_{16}(\text{PO}_4)_{15}\text{PO}_3\text{Cl}$	9.732	11.780	9.924	89.885	90.040	89.397

The crystal structure of $Pnma$ FePO_4 unit cell, the olivine-type LiFePO_4 delithiated form, is fully optimized. The lattice constant that we calculated with DFT+U are $a=4.88$, $b=5.92$, $c=9.98$ Å, separately, in satisfactory agreement with the experimental values¹ ($a = 4.788$, $b = 5.792$, and $c = 9.821$ Å) and the previous calculated values². Table S1 shows the lattice constant of $2 \times 2 \times 1$ supercell in the FePO_4 and doping systems by DFT+U

calculation. There are no extra electrons and holes in all the systems with structural optimization. All structural optimizations free up atomic positions and unit cell volumes.

C. Bader charge data of all systems.

Table S2. The Bader charge of all systems when forming a polaron at a special Fe atom.

	Fe ₁₆ P ₁₆ O ₆₄	Fe ₁₆ (PO ₄) ₁₅ AsO ₄	Fe ₁₆ (PO ₄) ₁₅ SeO ₄	Fe ₁₆ (PO ₄) ₁₅ SO ₄	Fe ₁₆ (PO ₄) ₁₅ SiO ₄	Fe ₁₆ (PO ₄) ₁₅ VO ₄	Fe ₁₆ (PO ₄) ₁₅ PO ₃ S	Fe ₁₆ (PO ₄) ₁₅ PO ₃ F	Fe ₁₆ (PO ₄) ₁₅ PO ₃ Cl
Fe-1	12.47	12.47	12.46	12.46	12.48	12.47	12.47	12.47	12.46
4	12.47	12.47	12.46	12.46	12.48	12.47	12.47	12.46	12.46
Fe-3	12.47	12.47	12.46	12.46	12.48	12.47	12.47	12.46	12.47
Fe-4	12.47	12.48	12.48	12.48	12.48	12.48	12.47	12.46	12.46
Fe-5	12.47	12.47	12.45	12.45	12.48	12.47	12.48	12.45	12.46
Fe-6	12.47	12.47	12.47	12.47	12.48	12.47	12.47	12.44	12.45
Fe-7	12.47	12.47	12.45	12.45	12.48	12.47	12.54	12.49	12.51
Fe-8	12.47	12.48	12.48	12.47	12.49	12.48	12.47	12.47	12.47
Fe-9	12.47	12.47	12.46	12.45	12.48	12.47	12.47	12.46	12.47
Fe-10	12.47	12.47	12.46	12.45	12.48	12.47	12.48	12.47	12.47
Fe-11	12.47	12.47	12.45	12.45	12.48	12.47	12.47	12.46	12.46
Fe-12	12.47	12.47	12.45	12.45	12.48	12.47	12.48	12.46	12.47
Fe-13	12.47	12.47	12.45	12.45	12.48	12.47	12.47	12.45	12.45
Fe-14	12.47	12.47	12.45	12.45	12.48	12.47	12.47	12.46	12.46
Fe-15	12.47	12.47	12.47	12.47	12.47	12.47	12.47	12.45	12.45
Fe-16	12.47	12.47	12.47	12.47	12.47	12.47	12.52	12.48	12.50

* Bader charge values of all other Fe atoms without polaron formation are about 12.06±0.02.

D. Bond length distortion when forming a polaron.

Table S3. The specific value of average bond length distortion Δ_i (i=1, 2, 3, 4, 5, 6) in the pristine and doping systems.

	Δ_1	Δ_2	Δ_3	Δ_4	Δ_5	Δ_6
$\text{Fe}_{16}\text{P}_{16}\text{O}_{64}$	0.06	0.06	0.11	0.11	0.11	0.11
$\text{Fe}_{16}(\text{PO}_4)_{15}\text{AsO}_4$	0.06	0.06	0.10	0.11	0.11	0.11
$\text{Fe}_{16}(\text{PO}_4)_{15}\text{SeO}_4$	0.06	0.06	0.09	0.10	0.11	0.11
$\text{Fe}_{16}(\text{PO}_4)_{15}\text{SO}_4$	0.06	0.06	0.09	0.10	0.11	0.11
$\text{Fe}_{16}(\text{PO}_4)_{15}\text{SiO}_4$	0.05	0.06	0.13	0.14	0.16	0.16
$\text{Fe}_{16}(\text{PO}_4)_{15}\text{VO}_4$	0.06	0.06	0.10	0.11	0.11	0.11
$\text{Fe}_{16}(\text{PO}_4)_{15}\text{PO}_3\text{S}$	0.05	0.06	0.10	0.10	0.11	0.12
$\text{Fe}_{16}(\text{PO}_4)_{15}\text{PO}_3\text{F}$	0.05	0.06	0.09	0.10	0.11	0.12
$\text{Fe}_{16}(\text{PO}_4)_{15}\text{PO}_3\text{Cl}$	0.05	0.06	0.09	0.10	0.11	0.12

To better compare the lattice distortions generated when different doping element pairs form polaron, we fixed the polaron on each Fe atom and calculated the corresponding Fe-O bond length distortion. The specific value of average bond length distortion was got by this equation:

$$\Delta_i = \frac{1}{16} \left(\sum_{j=1}^{16} (l_{ij}^{pol} - l_{ij}^{nopol}) \right) \quad (1)$$

Where l_{ij}^{nopol} is the index i of Fe-O bond length in FeO_6 when no polaron is fixed on the index j of Fe atom in the supercell. l_{ij}^{pol} is the i index of Fe-O bond length in FeO_6 when polaron is fixed on the index j of Fe atom in the supercell. The direction of the index i of Fe-O bond length in FeO_6 as shown in Figure 1c. Where the index j of Fe atom in the supercell is shown in Figure 1a.

E. All the data of E_{POL} .

Table S4. The polaron formation energy (E_{pol}) of the pristine and doped system at each Fe atom.

	$\text{Fe}_{16}\text{P}_{16}\text{O}_{64}$	$\text{Fe}_{16}(\text{PO}_4)_{15}$ AsO ₄	$\text{Fe}_{16}(\text{PO}_4)_{15}$ SeO ₄	$\text{Fe}_{16}(\text{PO}_4)_{15}$ SO ₄	$\text{Fe}_{16}(\text{PO}_4)_{15}$ SiO ₄	$\text{Fe}_{16}(\text{PO}_4)_{15}$ VO ₄	$\text{Fe}_{16}(\text{PO}_4)_{15}$ PO ₃ S	$\text{Fe}_{16}(\text{PO}_4)_{15}$ PO ₃ F	$\text{Fe}_{16}(\text{PO}_4)_{15}$ PO ₃ Cl
Fe-1	-0.298	-0.299	-0.144	-0.127	-0.583	-0.295	-0.331	-0.141	-0.137
Fe-2	-0.298	-0.304	-0.167	-0.138	-0.598	-0.315	-0.274	-0.114	-0.084
Fe-3	-0.298	-0.320	-0.196	-0.163	-0.547	-0.319	-0.350	-0.145	-0.158
Fe-4	-0.298	-0.280	-0.359	-0.363	-0.282	-0.279	-0.324	-0.116	-0.112
Fe-5	-0.298	-0.306	-0.197	-0.172	-0.517	-0.301	-0.374	-0.189	-0.223
Fe-6	-0.298	-0.276	-0.341	-0.341	-0.397	-0.346	-0.343	-0.214	-0.213
Fe-7	-0.298	-0.338	-0.244	-0.196	-0.518	-0.341	-0.288	-0.372	-0.416
Fe-8	-0.298	-0.316	-0.420	-0.363	-0.304	-0.363	-0.305	-0.290	-0.256
Fe-9	-0.298	-0.316	-0.205	-0.174	-0.554	-0.307	-0.312	-0.136	-0.124
Fe-10	-0.298	-0.316	-0.205	-0.175	-0.555	-0.308	-0.338	-0.203	-0.227
Fe-11	-0.298	-0.301	-0.181	-0.159	-0.571	-0.302	-0.349	-0.097	-0.109
Fe-12	-0.298	-0.301	-0.181	-0.159	-0.572	-0.302	-0.359	-0.113	-0.148
Fe-13	-0.298	-0.282	-0.210	-0.201	-0.521	-0.286	-0.322	-0.202	-0.187
Fe-14	-0.298	-0.282	-0.210	-0.201	-0.521	-0.286	-0.362	-0.175	-0.281
Fe-15	-0.298	-0.278	-0.302	-0.298	-0.424	-0.314	-0.307	-0.260	-0.162
Fe-16	-0.298	-0.278	-0.302	-0.298	-0.424	-0.314	-0.239	-0.380	-0.396
Average	-0.298	-0.300	-0.241	-0.220	-0.493	-0.311	-0.324	-0.197	-0.202

F. The data of Fe-O bond length at IS, TS, FS.

Table S5. The data of Fe-O bond length when polaron hopping between two adjacent Fe atoms in the pristine FePO_4 system.

	Fe-O bond length index	IS	TS	FS
Initial Fe atom	1	2.191	2.135	2.078
	2	2.191	2.147	2.103
	3	1.990	1.960	1.931
	4	2.277	2.167	2.056
	5	1.997	1.974	1.950
	6	2.277	2.258	2.240
Final Fe atom	1	1.934	1.961	1.989
	2	2.093	2.142	2.191
	3	2.007	2.098	2.191
	4	2.206	2.242	2.278
	5	1.958	1.977	1.997
	6	2.167	2.222	2.278

G. The data of polaron hopping rate.

The calculated polaron hopping rate (k_{et}) at room temperature (300 K) for all pathways in the pristine and doped system as shown in Table S6 and S7.

Table S6. The calculated polaron hopping rate (k_{et}) at room temperature (300 K) for all pathways in the pristine and P-site doped system. There are hopping rates for forward and reverse respectively along this path in doped system.

k_{et} (10^{10} Hz)	$\text{Fe}_{16}(\text{PO}_4)_{16}$	$\text{Fe}_{16}(\text{PO}_4)_{15}\text{AsO}_4$	$\text{Fe}_{16}(\text{PO}_4)_{15}\text{ScO}_4$	$\text{Fe}_{16}(\text{PO}_4)_{15}\text{SiO}_4$	$\text{Fe}_{16}(\text{PO}_4)_{15}\text{SO}_4$	$\text{Fe}_{16}(\text{PO}_4)_{15}\text{VO}_4$
upper Fe-1toFe-9	3.66	7.92 / 4.32	25.88 / 2.58	1.56 / 4.79	18.62 / 2.94	5.59 / 3.57
Fe-1toFe-10	3.66	8.25 / 4.49	25.88 / 2.58	1.56 / 4.81	18.71 / 2.97	6.83 / 4.39
Fe-1toFe-11	3.66	2.62 / 2.4	5.32 / 1.25	1.85 / 2.78	11.48 / 3.25	2.82 / 2.19

	Fe-1toFe-12	3.66	2.83 / 2.69	5.32 / 1.25	1.85 / 2.77	11.48 / 3.24	2.72 / 2.14
	Fe-2toFe-9	3.66	4.79 / 3.19	6.28 / 1.47	0.92 / 4.99	17.13 / 4.2	2.86 / 3.77
	Fe-2toFe-10	3.66	4.97 / 3.32	6.27 / 1.46	0.92 / 5.02	17.28 / 4.26	3.35 / 4.45
	Fe-2toFe-11	3.66	5.63 / 6.28	8.08 / 4.61	1.6 / 4.41	7.8 / 3.3	3.92 / 6.28
	Fe-2toFe-12	3.66	5.63 / 6.27	8.09 / 4.62	1.6 / 4.42	7.8 / 3.3	4.58 / 7.41
	Fe-3toFe-9	3.66	3.48 / 3.93	5.71 / 3.98	2.32 / 1.66	7.4 / 4.54	2.51 / 3.77
	Fe-3toFe-10	3.66	3.21 / 3.79	5.71 / 3.97	2.32 / 1.67	7.42 / 4.6	2.42 / 3.68
	Fe-3toFe-11	3.66	1.69 / 3.57	3.12 / 5.65	0.86 / 0.34	7.02 / 8.21	2.36 / 4.66
	Fe-3toFe-12	3.66	1.56 / 3.42	3.12 / 5.67	0.83 / 0.33	7.02 / 8.2	1.73 / 3.46
	Fe-4toFe-9	3.66	1.77 / 0.45	0.008 / 3.21	51.79 / 0.001	0.35 / 519.89	4.47 / 1.45
	Fe-4toFe-10	3.66	1.78 / 0.46	0.007 / 2.98	52.34 / 0.001	0.35 / 521.93	3.84 / 1.26
	Fe-4toFe-11	3.66	1.01 / 0.45	0.45 / 437.12	64.36 / 0.001	0.26 / 723.27	7.29 / 3.04
	Fe-4toFe-12	3.66	3.19 / 1.5	0.45 / 439.54	64.28 / 0.001	0.26 / 723.38	7.3 / 3.08
lower	Fe-5toFe-13	3.66	3.55 / 8.57	7.36 / 4.58	2.29 / 1.94	12.31 / 4.14	3.21 / 5.92
	Fe-5toFe-14	3.66	3.15 / 7.84	7.36 / 4.57	2.27 / 1.95	12.3 / 4.13	3.75 / 6.88
	Fe-5toFe-15	3.66	0.02 / 0.06	28.69 / 0.5	0.39 / 15.59	57.78 / 0.45	5.23 / 3.39
	Fe-5toFe-16	3.66	0.02 / 0.06	28.6 / 0.5	0.39 / 15.61	57.73 / 0.44	5.22 / 3.22
	Fe-6toFe-13	3.66	1.22 / 0.96	0.36 / 55.17	7.23 / 0.06	0.06 / 13.7	0.29 / 3.12
	Fe-6toFe-14	3.66	1.2 / 0.94	0.36 / 55.02	7.23 / 0.06	0.01 / 3.09	0.23 / 2.41
	Fe-6toFe-15	3.66	0.45 / 0.42	1.08 / 4.88	2.04 / 0.78	0.03 / 0.16	0.49 / 1.78
	Fe-6toFe-16	3.66	0.02 / 0.02	1.07 / 4.87	2.03 / 0.78	0.02 / 0.1	0.47 / 1.68
	Fe-7toFe-13	3.66	1.32 / 11.82	3.04 / 11.52	2.22 / 2.01	7.09 / 7.33	0.7 / 6.01
	Fe-7toFe-14	3.66	1.26 / 11.24	3.04 / 11.5	2.2 / 2.01	5.84 / 6.03	1.91 / 16.34
	Fe-7toFe-15	3.66	0.02 / 0.16	15.72 / 1.64	0.33 / 12.67	0.28 / 0.83	0.7 / 2.05
	Fe-7toFe-16	3.66	0.02 / 0.19	15.71 / 1.64	0.32 / 12.64	43.58 / 0.83	1 / 2.91
	Fe-8toFe-13	3.66	1.43 / 5.24	0.18 / 645.58	75.3 / 0.02	0.76 / 407.37	0.04 / 0.75
	Fe-8toFe-14	3.66	1.42 / 5.16	0.18 / 642.63	75.26 / 0.02	0.76 / 406.91	0.04 / 0.89
	Fe-8toFe-15	3.66	0.01 / 0.04	0.003 / 0.33	4.84 / 0.05	2.02 / 24.54	0.03 / 0.24
	Fe-8toFe-16	3.66	0.002 / 0.01	0.003 / 0.33	4.84 / 0.05	2.02 / 24.48	0.00003 / 0.002

Table S7. The calculated polaron hopping rate (k_{et}) at room temperature (300 K) for all pathways in the pristine and O-site doped system. There are hopping rates for forward and reverse respectively along this path in O-site doped system.

	k_{et} (10^{10} Hz)	$\text{Fe}_{16}(\text{PO}_4)_{16}$	$\text{Fe}_{16}(\text{PO}_4)_{15}\text{PO}_3\text{S}$	$\text{Fe}_{16}(\text{PO}_4)_{15}\text{PO}_3\text{F}$	$\text{Fe}_{16}(\text{PO}_4)_{15}\text{PO}_3\text{Cl}$
upper	Fe-1toFe-9	3.66	4.24 / 9.42	10.19 / 12.31	7.60 / 12.83
	Fe-1toFe-10	3.66	3.70 / 2.89	25.21 / 2.41	33.47 / 1.02
	Fe-1toFe-11	3.66	5.62 / 2.65	2.50 / 13.88	2.43 / 7.13

	Fe-1toFe-12	3.66	6.58 / 2.20	3.48 / 10.35	4.42 / 2.82
	Fe-2toFe-9	3.66	6.97 / 1.70	6.58 / 2.82	8.75 / 1.96
	Fe-2toFe-10	3.66	13.52 / 1.14	45.11 / 1.53	85.82 / 0.36
	Fe-2toFe-11	3.66	29.23 / 1.52	5.32 / 10.06	12.51 / 4.84
	Fe-2toFe-12	3.66	2.13 / 0.08	0.004 / 0.003	19.33 / 1.64
	Fe-3toFe-9	3.66	2.18 / 9.24	3.35 / 4.66	2.27 / 8.64
	Fe-3toFe-10	3.66	5.57 / 8.29	54.66 / 5.74	55.94 / 4.01
	Fe-3toFe-11	3.66	4.36 / 4.44	2.62 / 17.05	3.12 / 22.02
	Fe-3toFe-12	3.66	3.94 / 2.73	2.52 / 8.85	2.50 / 3.87
	Fe-4toFe-9	3.66	3.72 / 5.82	7.69 / 3.45	4.74 / 2.94
	Fe-4toFe-10	3.66	4.91 / 2.78	6.62 / 0.23	31.15 / 0.36
	Fe-4toFe-11	3.66	6.09 / 2.38	4.67 / 10.27	5.16 / 5.89
	Fe-4toFe-12	3.66	8.05 / 2.06	5.19 / 5.91	12.53 / 3.13
lower	Fe-5toFe-13	3.66	2.25 / 16.49	7.76 / 4.59	2.75 / 10.87
	Fe-5toFe-14	3.66	2.17 / 3.30	0.04 / 0.003	22.45 / 2.27
	Fe-5toFe-15	3.66	0.0006 / 0.01	5.87 / 10.14	2.18 / 23.49
	Fe-5toFe-16	3.66	0.07 / 13.50	440.28 / 0.28	236.11 / 0.30
	Fe-6toFe-13	3.66	3.19 / 7.25	6.91 / 10.67	4.66 / 12.98
	Fe-6toFe-14	3.66	3.92 / 1.84	0.44 / 0.08	29.35 / 2.11
	Fe-6toFe-15	3.66	0.32 / 1.28	3.56 / 16.23	0.80 / 5.89
	Fe-6toFe-16	3.66	0.10 / 5.57	422.81 / 0.69	153.64 / 0.13
	Fe-7toFe-13	3.66	0.35 / 0.10	0.07 / 48.43	0.004 / 25.28
	Fe-7toFe-14	3.66	3.63 / 0.21	0.02 / 1.73	0.02 / 4.05
	Fe-7toFe-15	3.66	1.03 / 0.52	0.08 / 161.57	0.001 / 24.41
	Fe-7toFe-16	3.66	2.82 / 18.79	0.05 / 0.04	0.26 / 0.55
	Fe-8toFe-13	3.66	9.28 / 4.79	1.35 / 40.69	1.94 / 28.13
	Fe-8toFe-14	3.66	18.28 / 2.02	2.17 / 6.96	5.60 / 2.06
	Fe-8toFe-15	3.66	2.50 / 2.35	0.42 / 34.92	0.46 / 16.48
	Fe-8toFe-16	3.66	0.11 / 1.35	5.10 / 0.15	17.17 / 0.07

H. Kinetic Monte Carlo simulation for small polaron hopping.

To more accurately evaluate the transition motions of polaron in the pristine and doped systems, we refer to previous research articles³⁻⁷ and perform Kinetic Monte Carlo (KMC) simulations for the pristine and doped systems using small polaron hopping rate. The specific implementation of the KMC algorithm is described as below:

1. Set up a lattice model with multiple sites represent different Fe atoms. A selected group of hopping between sites are considered in the simulation.

2. Calculate all non-equivalent hopping rates (between NN) k_{ab} from the method described in the Theory and computational methods for small polaron hopping rate at a specific temperature T , where a, b are sites.

3. Choose an arbitrary site as the starting point, marked as a .

4. Randomly choose the next site b to hop to: The probability to hop to the neighbor b_i is

$$p_i = \frac{k_{ab_i}}{\sum_j k_{ab_j}} .$$

A random number r_1 uniform distributed on $[0, 1)$ is generated. The site b_i is

chosen if $\sum_{j=1}^i p_j \leq r_1 < \sum_{j=1}^{i+1} p_j$.

5. A random number r_2 uniform distributed on $[0, 1)$ is generated, and the time cost

$$\Delta t = -\frac{\ln(r_2)}{\sum_i k_{ab_i}} .$$

Δt in this step is

6. Repeat the above two steps, and record the squared displacement L^2 and time per S steps until sampled M times, where S and M should be sufficiently large. The total simulation time is given by $MS\langle\Delta t\rangle$.

7. Repeat step 3 to 6 for N times, and take the average of these $L^2 - t$ curve (Each consists of M points). This would give an approximately linear or quadratic curve from which we can fit the diffusion coefficient D .

8. Repeat the above steps for K times and get a set of diffusion coefficient $D_i (i = 1, 2, \dots, K)$ and following mobility $\mu_i (i = 1, 2, \dots, K)$. We can estimate the error of the

mobility from this dataset as the Standard Deviation:
$$\sigma = \sqrt{\sum_{i=1}^K \frac{(\mu_i - \bar{\mu})^2}{K}}$$
.

For linear curve, meaning free hopping mode, the mean squared displacement (MSD) can be expressed as:

$$\langle L(t)^2 \rangle = 2ND t \quad (2)$$

where N is the dimensionality of the KMC process, D is the diffusion coefficient, $\langle L(t)^2 \rangle$ is the mean squared displacement and t is the time.

For nonlinear curve, meaning directed hopping mode, the mean squared displacement (MSD) can be expressed as:

$$\langle L(t)^2 \rangle = 2ND t + v^2 t^2 \quad (3)$$

where N is the dimensionality of the KMC process, D is the diffusion coefficient, v is the directional motion velocity and t is the time.

Afterward, we can obtain hopping mobility through the Einstein-Smoluchowski (ES) equation in the equation:

$$\mu^{ES} = \frac{qD}{k_B T} \quad (4)$$

Where k_B is Boltzmann constant and q is the carrier charge. We calculated the mean square displacement and time obtained by the KMC simulation, performed fitting to obtain

the diffusion mode and diffusion coefficient, and then used the Einstein relation to obtain the mobility.

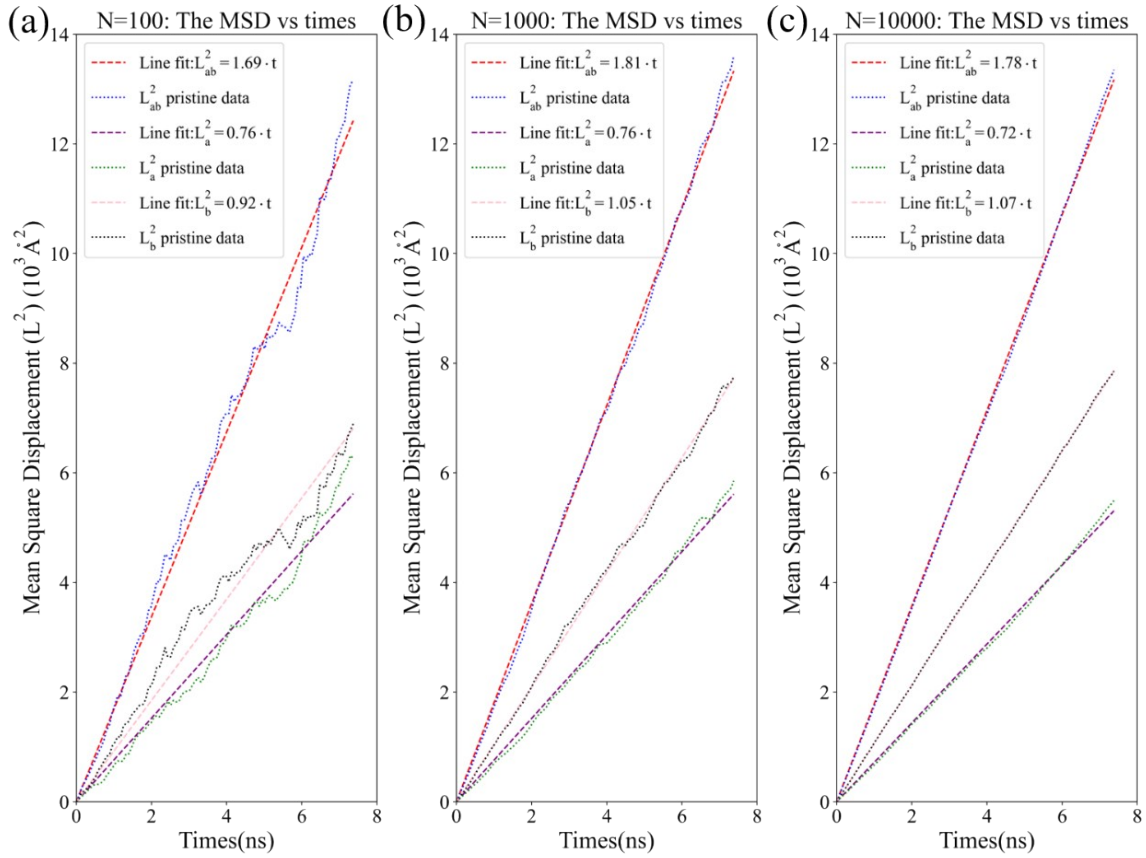


Figure S2: The mean square displacement (MSD) raw data and the fitted curve were obtained with times along the a and b axis from the KMC simulation, when N is (a) 100, (b) 1000, (c) 10000.

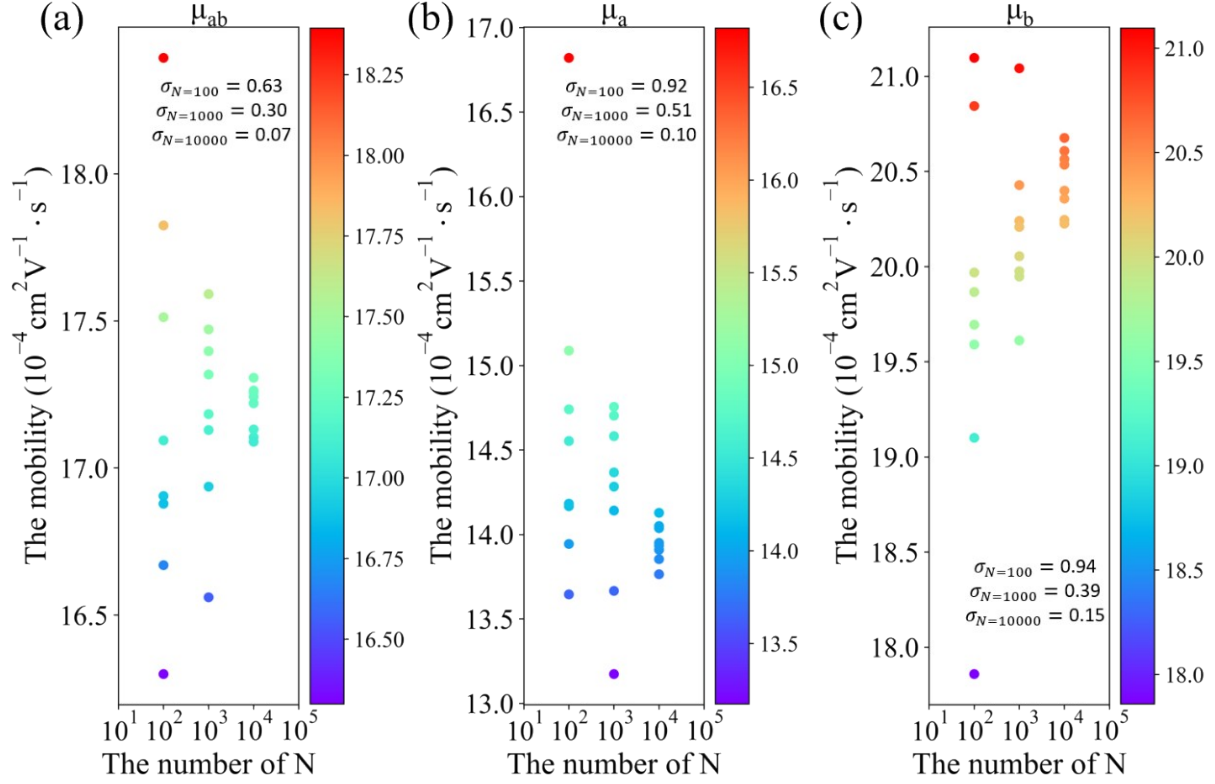


Figure S3: The polaron mobility in $\text{FeP}_{1-\alpha}\text{As}_\alpha\text{O}_4$ system obtained from different number of samplings N ($N=100, 1000, 10000$) along different axes: (a) ab-plane, (b) a-axis, (c) b-axis.

Here we listed results from the up layer of $\text{FeP}_{1-\alpha}\text{As}_\alpha\text{O}_4$ to illustrate the process. Figure S2 shows the average of square displacement over time of N samplings ($N=100, 1000, 10000$), along different axes, with $S=10$ and $M=100$. From Figure S2 we can see only with enough simulations ($N=10000$) there is a good linear relationship between L^2 and t . Figure S3 shows the mobility obtained from different number of samplings N ($N=100, 1000, 10000$), and for each N the simulation is repeated $K = 8$ times. The Standard Deviation is shown in Figure S3, which is smaller than 0.15 when $N = 10000$ which confirms the reliability of this simulation. It is clear that the instability decreases with increasing N .

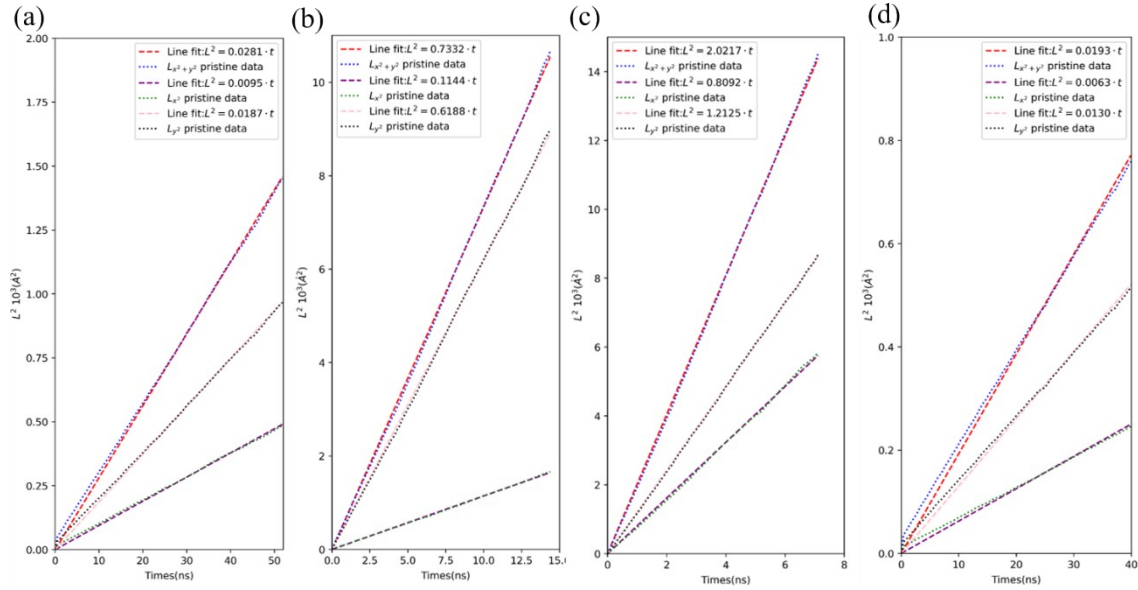


Figure S4. The mean square displacement (MSD) raw data and the fitted curve were obtained from the KMC simulation in the upper layer of (a) Se-doped, (b) Si-doped, (c) V-doped and (d) S-doped in P site system.

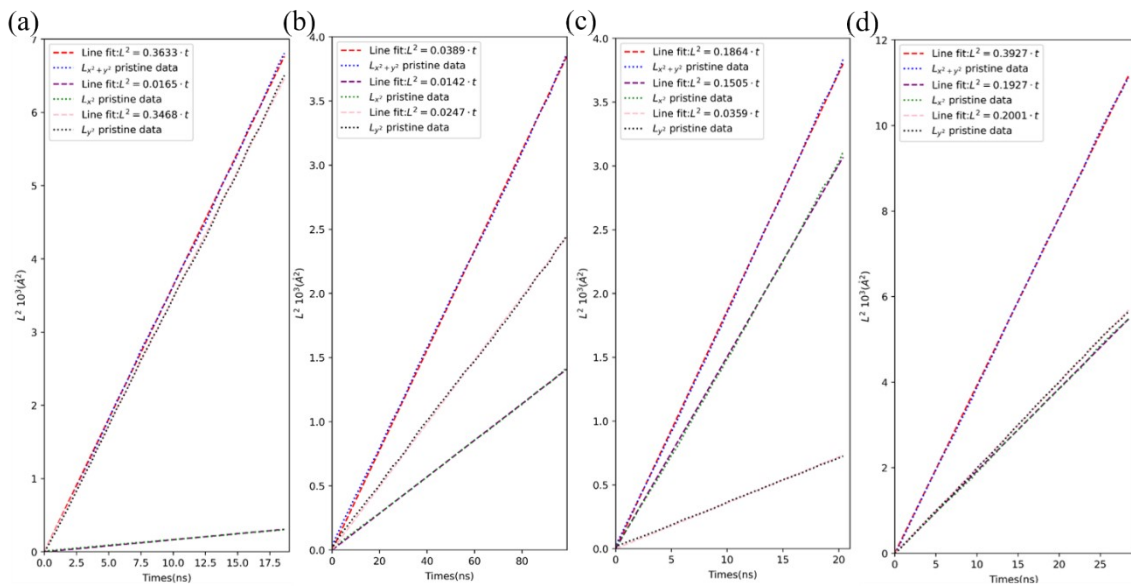


Figure S5. The mean square displacement (MSD) raw data and the fitted curve were obtained from the KMC simulation in the lower layer of (a) As-doped, (b) Se-doped, (c) Si-doped and (d) V-doped in P site system.

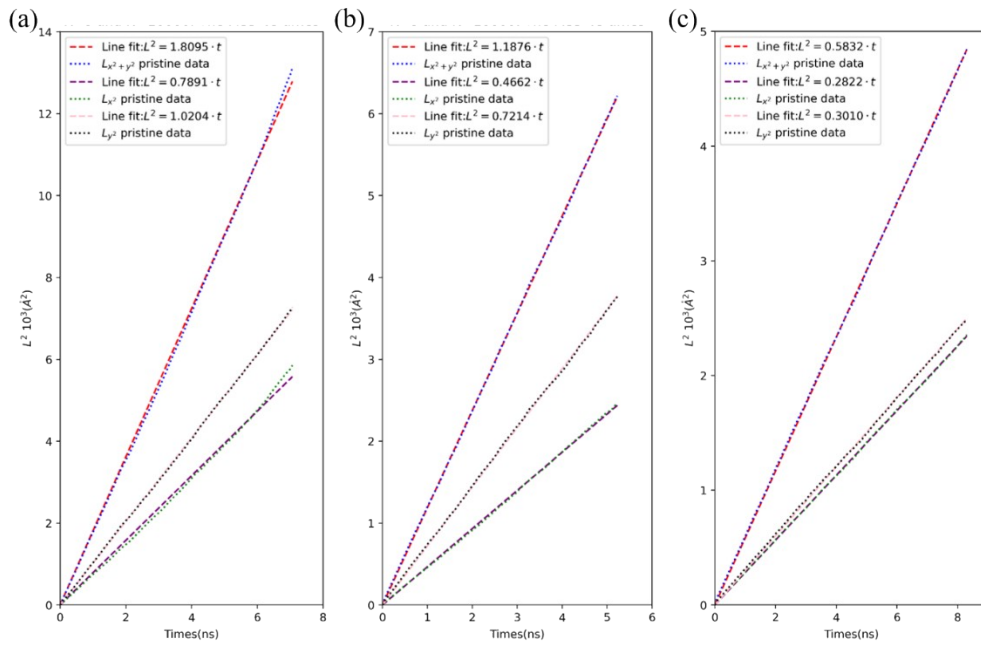


Figure S6. The mean square displacement (MSD) raw data and the fitted curve were obtained from the KMC simulation in the upper layer of (a) S-doped, (b) F-doped, and (c) Cl-doped in O site system.

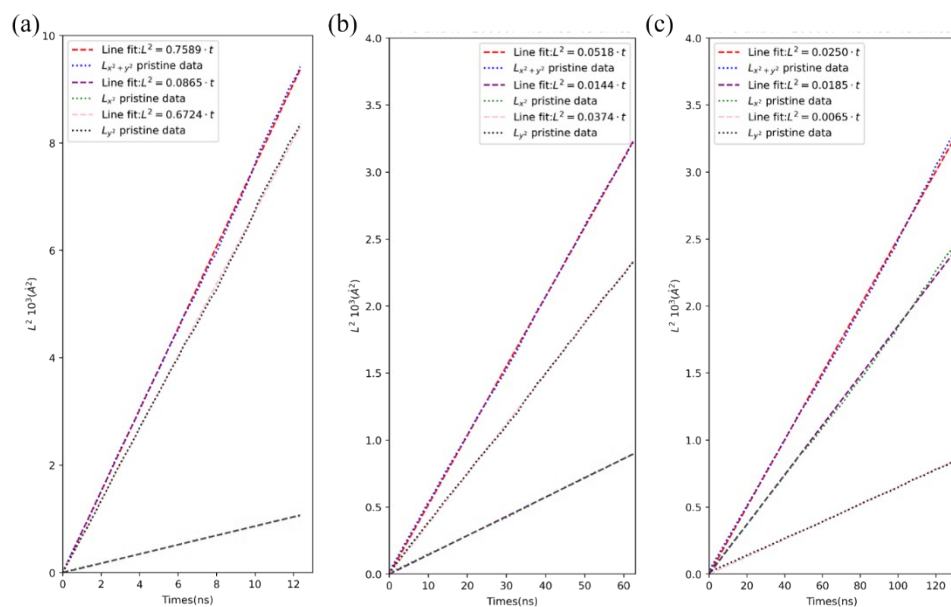


Figure S7. The mean square displacement (MSD) raw data and the fitted curve were obtained from the KMC simulation in the lower layer of (a) S-doped, (b) F-doped, and (c) Cl-doped in O site system.

REFERENCES

1. A. K. Padhi, K. S. Nanjundaswamy and J. B. Goodenough, *J. Electrochem. Soc.*, 1997, **144**, 1188-1194.
2. T. Maxisch, F. Zhou and G. Ceder, *Physical Review B*, 2006, **73**, 104301.
3. V. Pasumarthi, T. Liu, M. Dupuis and C. Li, *J. Mater. Chem. A*, 2019, **7**, 3054-3065.
4. F. Wu and Y. Ping, *J. Mater. Chem. A*, 2018, **6**, 20025-20036.
5. L. Vittadello, M. Bazzan, S. Messerschmidt and M. Imlau, *Crystals*, 2018, **8**.
6. T. Liu, V. Pasumarthi, C. LaPorte, Z. Feng, Q. Li, J. Yang, C. Li and M. Dupuis,

J. Mater. Chem. A, 2018, **6**, 3714-3723.

7. I. Mhaouech and L. Guilbert, *Solid State Sci.*, 2016, **60**, 28-36.